Research on Per-cell Codebook based Channel Quantization for CoMP Transmission

Zhirui Hu[1], Chunyan Feng[1], Tiankui Zhang[1], Qiubin Gao[2], Shaohui Sun[2]
[1]Beijing Key Laboratory of Network System Architecture and Convergence,
Beijing University of Posts and Telecommunications Beijing, China
[e-mail: huzhirui74@163.com, tkzhang@gmail.com]
[2]State Key Laboratory of Wireless Mobile Communications (CATT),
Beijing, China
[e-mail: gaoqiubin@catt.cn]
*Corresponding author: Tiankui Zhang

Received January 7, 2014; revised April 13, 2014; accepted May 6, 2014; published June 27, 2014

Abstract

Coordinated multi-point (CoMP) transmission has been regarded as a potential technology for LTE-Advanced. In frequency division duplexing systems, channel quantization is applied for reporting channel state information (CSI). Considering the dynamic number of cooperation base stations (BSs), asymmetry feature of CoMP channels and high searching complexity, simply increasing the size of the codebook used in traditional multiple antenna systems to quantize the global CSI of CoMP systems directly is infeasible. Per-cell codebook based channel quantization to quantize local CSI for each BS separately is an effective method. In this paper, the theoretical upper bounds of system throughput are derived for two codeword selection schemes, independent codeword selection (ICS) and joint codeword selection (JCS), respectively. The feedback overhead and selection complexity of these two schemes are analyzed. In the simulation, the system throughput of ICS and JCS is compared. Both analysis and simulation results show that JCS has a better tradeoff between system throughput and feedback overhead. The ICS has obvious advantage in complexity, but it needs additional phase information (PI) feedback for obtaining the approximate system throughput with JCS. Under the same number of feedback bits constraint, allocating the number of bits for channel direction information (CDI) and PI quantization can increase the system throughput, but ICS is still inferior to JCS. Based on theoretical analysis and simulation results, some recommendations are given with regard to the application of each scheme respectively.

Keywords: CoMP system, channel quantization, limited feedback, per-cell codebook, codeword selection, bits allocation

http://dx.doi.org/10.3837/tiis.2014.06.001

1. Introduction

To achieve the required peak data rates up to 1 Gbit/s for low mobility and 100 Mbit/s for high mobility in the 4G standards, a straightforward method is to increase the transmission antennas, e.g., the long term evolution (LTE) system allows for up to 8 antenna ports at the base station (BS). However, it is challenging for antenna configurations, especially for the situation with large scale antenna arrays [1]. Another way to increase the transmission antennas is coordinated multi-point (CoMP) transmission, a kind of distributed antenna systems [2] or named as network multi-input multi-output (MIMO), which employs BS cooperation among the neighboring cells for joint signal transmission, taking advantage of the distributed multiple antennas to achieve spatial multiplexing gain or transmit diversity gain. It has been considered as one of the potential technologies for LTE-Advanced [3][4].

CoMP transmission is divided into coordinated scheduling/beamforming (CS/CB) and joint processing (JP). In CS/CB, data is only transmitted from a single BS [5][6], but coordination BSs exchange channel state information (CSI) with each other, so that scheduling can be performed to reduce inter-cell interference. In JP, data is simultaneously transmitted from coordination BSs, requring all coordination BSs to share data and CSI. This paper focuses on JP system, and CoMP refers in particular to JP below.

The gain of CoMP system largely depends on the availability of CSI at BSs. In practical, the CSI may be available due to the channel reciprocity for time division duplexing systems. But for frequency division duplexing systems, channel quantization at user equipment (UE) is needed to report CSI. Relative to MIMO systems, the acquirement of CSI at BS is more challenging, as UE should report CSI of all cooperation BSs [7]. It is a heavy burden for the low-capacity feedback links.

In general, a predefined codebook is designed for channel quantization by vector quantization theory, based on which, the UE quantizes CSI and feeds back the index of the codeword to the BS [8]. Since UE should feedback the CSI of all the cooperation BSs in CoMP system, the codebook for CSI quantization should be studied [9]. An intuitive method is to design a large size codebook by treating the cooperation BSs as a super BS, which is named as the joint-cell codebook approach [10]. The joint-cell codebook method is optimal. However, in the practical system, the method is infeasible because of the asymmetry feature of CoMP channels, high searching complexity and varying codebook size caused by the dynamic number of cooperation BSs [11]. Therefore, the per-cell codebook method for CSI quantization has drawn much attention, in which each cooperation BS has an independent codebook [11-17]. The codebook designed for single-cell MIMO system can be used for per-cell codebook for CoMP system as well.

When UE uses the per-cell codebook scheme, there are different codeword selection schemes. [9] proposed two codeword selection schemes, joint codeword selection (JCS) and independent codeword selection (ICS), and analyzed the complexity of these two schemes. For JCS, the codewords are selected jointly to minimize the quantization error of the cooperation cells channel direction information (CDI), and ICS is to minimize the quantization error of single cell CDI with the codewords selected independently for cooperation BSs. JCS is superior to ICS in system throughput. However, the complexity of the codeword selection is high. Since the preferred codeword for each BS is obtained by exhaustive search over all the codebooks of the multiple cells, JCS has exponential complexity with respect to (w.r.t.) the size of the codebook. [12] proposed a codebook compression scheme to reduce the complexity

of JCS. By selecting suitable codewords from original codebooks, the sub-codebooks with smaller size are combined for CDI quantization.

Conversely, the selection complexity of ICS is low, but the phase ambiguity (PA) derived from the per-cell quantization degrades the system performance, including distributed array gain, macro diversity gain and normalized quantization gain [13-15]. The authors of [13][14] had proved that the received signal to noise ratio (SNR) approaches zero with probability 1 when the number of the coordinated BSs approximates infinity, even though the codebook size is asymptotically large. [15] pointed that only for cell edge users, the PA will lead to significant performance degradation of the joint CDI quantization. Therefore, [16] proposed a new quantization technique to solve the PA problem, where the quantization of each of the real and the imaginary parts is performed independently using the same real codebook. Additionally, feeding back a few phase information (PI) bits in each cell for PA is an effective way to compensate the performance loss [17][18], even 1-bit PI feedback can greatly increase the system performance [13]. [17] analyzed the average quantization performance of ICS with or without PI feedback, and showed the necessity of the PI quantization especially for cell-edge users. [18] quantified the specific required bits number for PI quantization to ensure an allowed quantization error loss. However, the introduction of the PI feedback will increase the control information feedback and overhead.

Under the total number of feedback bits constraint, rational allocating the number of feedback bits for CDI and PI quantization can improve the system performance without increasing the feedback overhead [18][19]. In [19], a bit allocation scheme, by maximizing quantization accuracy, was proposed and derived the solution by searching the possible bit combinations. [18] derived closed-form solutions of the allocated feedback bits for CDI and PI quantization. The scheme to allocate feedback bits between CDI and PI for relay system, aimed at maximizing UE's rate, is given in [20]. Besides CDI and PI, feedback-bit allocation among users is also needed for multi-user (MU) systems [21]. [22] concluded that users with higher requested quality-of-service, i.e., lower outage probabilities and higher downlink rates, should use larger shares of the feedback rate. The feedback-bit allocation algorithm among users can offer a 20% performance gain over the equal bit allocation scheme [23].

The above researches proposed two codeword selection schemes, JCS and ICS, without analyzing the different effect on system throughput. For ICS, the necessity and effectiveness of PI feedback for improving quantization accuracy had been analyzed. However, the performance of ICS with PI feedback (called for ICS below) and JCS are not compared comprehensively. In this paper, we study JCS and ICS for channel quantization based on the per-cell codebook in CoMP system. Several respects of ICS and JCS, including feedback overhead, selection complexity and system throughput, are compared. For ICS, the scheme of optimal feedback-bit allocation by maximizing system throughput is given. The numerical and simulation results are given to verify the theoretical system throughput. With regard to the problems of each scheme found through theoretical analysis and simulation results, some recommendations, selection complexity reducing for JCS and feedback-bit allocation for ICS, are given at last in the paper.

The contributions of the paper are summarized as follows.

- We derive the upper bounds of system throughput of two codeword selection schemes, JCS and ICS, both in SU and MU scenarios for CoMP system. The system throughput upper bound is a function of the number of feedback bits for CDI quantization. When PA is considered for ICS, the system throughput upper bound of ICS is also a function of the number of feedback bits for PI quantization.

- We compare the throughput of JCS and ICS by Monte Carlo simulation. We also compare JCS and ICS in feedback overhead and selection complexity. While JCS has higher selection complexity, ICS has higher feedback overhead.
- According to the feature of JCS and ICS analyzed in this paper, we give some recommendations with regard to the application of each scheme respectively.

This paper gives the upper bounds of system throughput of JCS and ICS. However, for ICS, the solution of feedback-bit allocation by maximizing the system throughput is derived by exhaustively searching. The close-form expression of the number of feedback-bit will be solved in the future work.

As for notations, we use uppercase boldface letters to denote matrices and lowercase boldface to denote vectors. The operators $(\cdot)^T, (\cdot)^H, (\cdot)^\dagger$ stand for transpose, Hermitian and pseudo-inverse respectively. $\mathbf{E}(\cdot)$ is the expectation operator. $\|\cdot\|$ represents norm operation.

2. System Description

2.1 System Model of CoMP Joint Processing

Consider a CoMP system with N BSs, each equipped with n_t antennas, cooperatively serving K single-antenna UEs. The nearest BS to the kth UE is the serving BS, and the other $N-1$ BSs are the coordinated BSs for UE k. As shown in **Fig.1**, N BSs cooperatively serve the UE k.

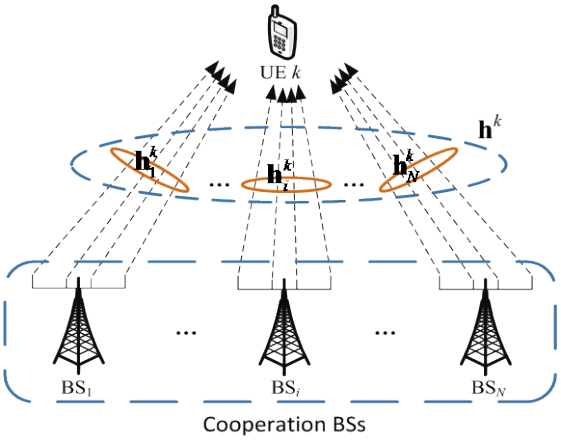

Fig. 1. An example of CoMP system. The dotted lines with arrow denote wireless links.

As to the UE k, the N cooperation BSs seem as a virtual super BS with Nn_t antennas. Similarly, the channel vector between the virtual super BS and UE k (called "global CSI", denote $\mathbf{h}^k$ in Fig.1) with $1\times Nn_t$ dimension is the combination of the single cell channel vectors (called "local CSI", denote $\mathbf{h}_1^k, \cdots \mathbf{h}_i^k \cdots, \mathbf{h}_N^k$ in Fig.1). Therefore, the global CSI for UE k can be expressed by

$$\mathbf{h}^k = \left[\alpha_1^k \mathbf{h}_1^k, \cdots, \alpha_i^k \mathbf{h}_i^k, \cdots, \alpha_N^k \mathbf{h}_N^k\right] \tag{1}$$

where $\alpha_i^k \left(i = 1, \cdots, N\right)$ is the large scale fading gain including path loss and shadowing component, $\mathbf{h}_i^k \in C^{1\times n_t}$ is local CSI from the ith BS to UE k, whose entries are independent and

identically distributed (i.i.d.) complex Gaussian variables with zero mean and unit variance.

We assume that the transmit power P is uniformly allocated to K UEs, that is, the transmit power of each BS for UE k is $p = P/K$. The received signal of the kth UE is

$$y_k = \sqrt{p}\mathbf{h}^k\hat{\mathbf{v}}^k x_k + \sum_{t=1,t\neq k}^{K}\sqrt{p}\mathbf{h}^k\hat{\mathbf{v}}^t x_t + n_k = \sum_{i=1}^{N}\sqrt{p}\mathbf{h}_i^k\hat{\mathbf{v}}_i^k x_k + \sum_{t=1,t\neq k}^{K}\sum_{i=1}^{N}\sqrt{p}\mathbf{h}_i^k\hat{\mathbf{v}}_i^t x_t + n_k \tag{2}$$

where $\hat{\mathbf{v}}^k = \left[\left(\hat{\mathbf{v}}_1^k\right)^T,\cdots,\left(\hat{\mathbf{v}}_N^k\right)^T\right]^T$ is the precoding vector for UE k, $\hat{\mathbf{v}}_i^k \in C^{n_t\times 1}$ is the precoding of the ith BS with power constraint $\left\|\hat{\mathbf{v}}_i^k\right\| = 1$, which is obtained according to the limited feedback information (details in Section 2.2). x_k is the transmitted signal of UE k. The second term on the right-hand side of (2) is the MU interference, and n_k is Gaussian noise variable with zero mean and σ^2 variance.

2.2 Characteristics of Global CDI

From the structure of the global CSI shown in (1), we can conclude that the global CSI is no longer i.i.d. due to the existence of the heterogeneous large scale fading gains of multiple single cell channels.

The CDI of the global CSI is

$$\tilde{\mathbf{h}}^k = \left[\tilde{\mathbf{h}}_1^k,\cdots,\tilde{\mathbf{h}}_i^k,\cdots,\tilde{\mathbf{h}}_N^k\right] = \mathbf{h}^k\Big/\left\|\mathbf{h}^k\right\| = \frac{1}{\sqrt{\sum_{i=1}^{N}\left(\alpha_i^k\right)^2\left\|\mathbf{h}_i^k\right\|^2}}\left[\alpha_1^k\mathbf{h}_1^k,\cdots,\alpha_i^k\mathbf{h}_i^k,\cdots,\alpha_N^k\mathbf{h}_N^k\right] \tag{3}$$

We assume $\left\|\mathbf{h}_i^k\right\|$ and $\bar{\mathbf{h}}_i^k$ are the channel magnitude information and CDI of $\mathbf{h}_i^k$ respectively, that is, $\mathbf{h}_i^k = \left\|\mathbf{h}_i^k\right\|\bar{\mathbf{h}}_i^k$. (3) can be rewritten as

$$\tilde{\mathbf{h}}^k = \frac{\left[\alpha_1^k\left\|\mathbf{h}_1^k\right\|\bar{\mathbf{h}}_1^k,\cdots,\alpha_i^k\left\|\mathbf{h}_i^k\right\|\bar{\mathbf{h}}_i^k,\cdots,\alpha_N^k\left\|\mathbf{h}_N^k\right\|\bar{\mathbf{h}}_N^k\right]}{\sqrt{\sum_{i=1}^{N}\left(\alpha_i^k\right)^2\left\|\mathbf{h}_i^k\right\|^2}} \triangleq \left[g_1^k\bar{\mathbf{h}}_1^k,\cdots,g_i^k\bar{\mathbf{h}}_i^k,\cdots,g_N^k\bar{\mathbf{h}}_N^k\right] \triangleq \bar{\bar{\mathbf{h}}}^k\mathbf{G}^k \tag{4}$$

where $\bar{\bar{\mathbf{h}}}^k = \left[\bar{\mathbf{h}}_1^k,\cdots,\bar{\mathbf{h}}_i^k,\cdots,\bar{\mathbf{h}}_N^k\right]$ is an aggregation of the CDI of local CSI, $g_i^k \triangleq \alpha_i^k\left\|\mathbf{h}_i^k\right\|\Big/\sqrt{\sum_{i=1}^{N}\left(\alpha_i^k\right)^2\left\|\mathbf{h}_i^k\right\|^2}$ is the ith channel gain of user k, and $\mathbf{G}^k = diag\left\{g_1^k,\cdots,g_N^k\right\}$ is the channel gain matrix of user k.

Expression (4) implies that the CDI of global CSI has the following characteristics.

- It is not the simple combination of local CDI $\bar{\bar{\mathbf{h}}}^k$. It also depends on the channel gain matrix $\mathbf{G}^k$, which results in the entries of $\tilde{\mathbf{h}}^k$ being no longer i.i.d..
- The ratio between different BSs' channel gain $g_i^k/g_j^k = \alpha_i^k/\alpha_j^k\,(i\neq j)$ varies frequently and is fluctuant in a large range when UEs move, especially with high-speed, as α_j^k is highly depends on UE's location.

- Under the scenario of dynamic cooperation cells, the cooperation sets of cells for each UE is dynamically adjusted according to the predefined criterion, in other words, N is varies from UEs and with time, as which the dimension of $\tilde{\mathbf{h}}^k \in C^{1\times Nn_t}$ is not fixed.

2.3 Per-cell Codebook based CDI Quantization

In the limited feedback system, CSI quantization is processed at UE before reported to BS. In order to highlight the impact of codebook on CDI quantization, we assume that the large scale fading gain $\alpha_i^k \left(i=1,\cdots,N\right)$ and the small scale fading channel norm $\left\|\mathbf{h}_i^k\right\|, i=1,\cdots,N$ are perfectly obtained at BSs.

The kth UE is assumed to have perfect and instantaneous knowledge of $\mathbf{h}_i^k, i=1,2,\cdots,N$. Codebook is necessary for CDI quantization, which is fixed beforehand and is known to both the BSs and the UEs. With per-cell codebook, the CDI of each BS is quantized to one of the codewords in the codebook for each BS, and the index of each selected codeword is perfectly fed back from the UE to the serving BS. Then, each BS uses the codeword corresponding to the index as the CDI. Assume that $\hat{\mathbf{h}}_i^k$ is the quantized version of $\bar{\mathbf{h}}_i^k$ and $\bar{\bar{\mathbf{h}}}'^k = \left[\hat{\mathbf{h}}_1^k,\cdots,\hat{\mathbf{h}}_N^k\right]$, the global CDI obtained at BSs can be reconstructed as

$$\hat{\mathbf{h}}^k = \left[g_1^k\hat{\mathbf{h}}_1^k,\cdots,g_i^k\hat{\mathbf{h}}_i^k,\cdots,g_N^k\hat{\mathbf{h}}_N^k\right] = \bar{\bar{\mathbf{h}}}'^k\mathbf{G}^k \tag{5}$$

Assume that the per-cell quantization codebook for each BS is denoted as $C_i\left(i=1,\cdots,N\right)$, which consists of unit norm vectors $\mathbf{c}_{ij}\left(j=1,\cdots,2^{B_c}\right)$ in $C^{n_t\times 1}$, and B_c is the number of feedback bits allocated to each BS.

We use the minimum chordal distance criterion to quantize the vectors. The criterion for ICS $\hat{\mathbf{h}}_i^k = Q_{ICS}\left(\bar{\mathbf{h}}_i^k\right)$ can be expressed as

$$Q_{ICS}\left(\bar{\mathbf{h}}_i^k\right) = \arg\max_{\mathbf{c}_{ij}\in C_i}\left\|\bar{\mathbf{h}}_i^k\mathbf{c}_{ij}^H\right\|, \quad i=1,\cdots,N \tag{6}$$

while the JCS $\left(\hat{\mathbf{h}}_1^k,\hat{\mathbf{h}}_2^k,\cdots,\hat{\mathbf{h}}_N^k\right) = Q_{JCS}\left(\tilde{\mathbf{h}}^k\right)$ follows the criterion of

$$Q_{JCS}\left(\tilde{\mathbf{h}}^k\right) = \arg\max_{\mathbf{c}_{ij}\in C_i}\left\|\sum_{i=1}^{N}\tilde{\mathbf{h}}_i^k\mathbf{c}_{ij}^H\right\| \tag{7}$$

In the following, we assume that the random vector quantization codebook is used. Therefore, each of the vectors within C_i is selected randomly and independently from the uniform distribution on the complex unit sphere. We analyze the performance averaged over all such choices of random codebooks.

Define $D\left(2^{B_c},n_t\right) = \mathrm{E}\left(\left\|\bar{\mathbf{h}}_i^k\left(\hat{\mathbf{h}}_i^k\right)^H\right\|^2\right)$ as the average quantization accuracy, which is [24]

$$D\left(2^{B_c},n_t\right) = 1-2^{B_c}\beta\left(2^{B_c},\frac{n_t}{n_t-1}\right) \tag{8}$$

where $\beta(\cdot,\cdot)$ is the Beta function. It is also shown in [24] that $D\left(2^{B_c}, n_t\right)$ is tightly bounded as

$$1-2^{-\frac{B_c}{n_t-1}} \le D\left(2^{B_c}, n_t\right) \le 1-\frac{n_t-1}{n_t}2^{-\frac{B_c}{n_t-1}} \tag{9}$$

In order to facilitate the description, the codebook size for JCS and ICS is denoted as $2^{B_c^J}$ and $2^{B_c^I}$, respectively.

3. Performance Analysis of CDI Quantization

In this section, we analyze the performance of CDI quantization with two codeword selection schemes, ICS and JCS. The theoretical upper bounds of system throughput are derived for ICS and JCS both in SU and MU situation. Then we compare the two schemes in the feedback overhead and selection complexity.

3.1 Throughput Analysis

3.1.1 SU scenario (*K*=1)

In this scenario, there is no MU interference, that is, the received signal of the UE comprises of the first and the third term in the right-hand side of (2). In this sector, all of the superscript *k* on variables in previous sectors is replaced by 1.

For per-cell codebook based limited feedback, the system throughput is given by

$$R^1 = \mathrm{E}\log_2\left(1+\rho\left|\sum_{i=1}^{N}\alpha_i^1\mathbf{h}_i^1\hat{\mathbf{v}}_i^1\right|^2\right) \tag{10}$$

where ρ denotes the ratio between the transmit power of each BS for each UE and the noise variance, i.e. $\rho = p/\sigma^2$. The superscript 1 on R is taken to state the expression denoting the throughput for the system with K=1 UE.

In this situation, maximum ratio transmission is adopted to boost the signal power. Therefore, $\hat{\mathbf{v}}_i^1$ is a quantized vector of $\bar{\mathbf{h}}_i^1$, that is, $\hat{\mathbf{v}}_i^1 = \left(\hat{\mathbf{h}}_i^1\right)^H$. Then, the precoding vector of the UE can be denoted as $\hat{\mathbf{v}}^1 = \left[\hat{\mathbf{h}}_1^1,\cdots,\hat{\mathbf{h}}_N^1\right]^H$. As all of the quantized variables $\hat{\mathbf{h}}_1^1,\cdots,\hat{\mathbf{h}}_N^1$ have unit norm, we can achieve $\left\|\hat{\mathbf{v}}^1\right\| = \sqrt{N}$.

In order to analyze the system throughput of JCS with per-cell codebook, we first state a lemma demonstrated in [11], i.e., JCS with per-cell codebook scheme and joint-cell codebook scheme can achieve the same average quantization accuracy with sufficiently large n_t and finite N. Assume that $\breve{\mathbf{h}}^k = \left[\breve{\mathbf{h}}_1^k,\cdots,\breve{\mathbf{h}}_N^k\right]$ with unit norm is the combination of the quantized CDIs selected from the joint-cell codebook, which consists of $2^{NB_c^J}$ entries in $Nn_t \times 1$ [9]. So the average quantization accuracy of JCS can be given by

$$\mathrm{E}\left(\left|\tilde{\mathbf{h}}^1\left(\hat{\mathbf{h}}^1\right)^H\right|^2\right)=\mathrm{E}\left(\left\|\hat{\mathbf{h}}^1\right\|\tilde{\mathbf{h}}^1\left(\breve{\mathbf{h}}^1\right)^H\right|^2\right)=N\cdot\mathrm{E}\left(\left|\tilde{\mathbf{h}}^1\left(\breve{\mathbf{h}}^1\right)^H\right|^2\right) \tag{11}$$

The system throughput of JCS can be obtained by

$$\begin{aligned}R_{JCS}^1&=\mathrm{E}\log_2\left(1+\rho\left|\mathbf{h}^1\hat{\mathbf{v}}^1\right|^2\right)\overset{(a)}{\le}\log_2\left(1+\rho\,\mathrm{E}\left\|\mathbf{h}^1\right\|^2\cdot\mathrm{E}\left|\tilde{\mathbf{h}}^1\left(\hat{\mathbf{h}}^1\right)^H\right|^2\right)\\&\overset{(b)}{=}\log_2\left(1+\rho\,\mathrm{E}\left\|\mathbf{h}^1\right\|^2\cdot N\cdot\mathrm{E}\left|\tilde{\mathbf{h}}^1\left(\breve{\mathbf{h}}^1\right)^H\right|^2\right)\\&\overset{(c)}{=}\log_2\left(1+\rho N\,\mathrm{E}\left\|\mathbf{h}^1\right\|^2\cdot D\left(2^{NB_c^1},Nn_t\right)\right)\end{aligned} \tag{12}$$

Here, (a) follows Jensen's inequality and by substituting $\mathbf{h}^1=\left\|\mathbf{h}^1\right\|\tilde{\mathbf{h}}^1$ for $\mathbf{h}^1$. (b) is satisfied by using (11). Step (c) is arrived at by noting that $\left\|\mathbf{h}^1\right\|^2$ is independent with $\tilde{\mathbf{h}}^1$ and the use of (8). Finally, substituting (9) in (12), we get the upper bound of the system throughput of the JCS

$$R_{JCS}^1\le\log_2\left(1+\rho N\,\mathrm{E}\left\|\mathbf{h}^1\right\|^2\cdot\left(1-\frac{Nn_t-1}{Nn_t}2^{-\frac{NB_c}{Nn_t-1}}\right)\right) \tag{13}$$

For the special case where $\alpha_1^1=\cdots=\alpha_N^1=\alpha^1$, corresponding to some cell edge UE, (13) can be derived as

$$R_{JCS}^{1-edge}\le\log_2\left(1+\rho N^2n_t\left(\alpha^1\right)^2\cdot\left(1-\frac{Nn_t-1}{Nn_t}2^{-\frac{NB_c}{Nn_t-1}}\right)\right) \tag{14}$$

since $\left\|\mathbf{h}^1\right\|^2=\left(\alpha^1\right)^2\sum_{i=1}^N\left\|\mathbf{h}_i^1\right\|^2$ and $\left\|\mathbf{h}_i^1\right\|^2$ is chi-square with n_t degrees of freedom.

Different from JCS, the codewords selected by ICS aim to maximum the quantization accuracy for each local CSI. However, it cannot guarantee the maximum of the received signal power on account of the existence of PA, which is caused by the property of the selection criterion,

$$Q_{ICS}\left(\bar{\mathbf{h}}_i^k\right)=Q_{ICS}\left(\bar{\mathbf{h}}_i^k\cdot e^{j\theta}\right) \tag{15}$$

where θ is an arbitrary phase rotation. The received signal power can be written as

$$\left|\sum_{i=1}^N\alpha_i^1\mathbf{h}_i^1\hat{\mathbf{v}}_i^1\right|^2=\left|\sum_{i=1}^N\alpha_i^1\left\|\mathbf{h}_i^1\right\|\bar{\mathbf{h}}_i^1\left(\hat{\mathbf{h}}_i^1\right)^H\left|e^{j\theta_i}\right|^2\right. \tag{16}$$

where θ_i (called PI in this paper) is the phase of $\mathbf{h}_i^1\hat{\mathbf{v}}_i^1$. It shows that the received signal not

only depends on quantization accuracy $\left|\overline{\mathbf{h}}_i^1\left(\hat{\mathbf{h}}_i^1\right)^H\right|$, but related to the phase θ_i. The phase differences between $\theta_i\,(i=1,\cdots,N)$ lower the power of the received signal. Feedback quantization version of θ_i can reduce the effect of PI. Denote $\hat{\theta}_i$ as the quantization of θ_i with B_{PI} bits, then $\Delta\theta_i=\theta_i-\hat{\theta}_i$ is the PI quantization error. The average received signal power is computed as follows.

$$\begin{aligned}\mathrm{E}\left|\sum_{i=1}^{N}\alpha_i^1\mathbf{h}_i^1\hat{\mathbf{v}}_i^1\right|^2&=\mathrm{E}\left|\sum_{i=1}^{N}\alpha_i^1\left\|\mathbf{h}_i^1\right\|\overline{\mathbf{h}}_i^1\left(\hat{\mathbf{h}}_i^1\right)^H\left|e^{j\Delta\theta_i}\right|^2\overset{(a)}{\approx}n_tD\left(2^{B_c^I},n_t\right)\mathrm{E}\left|\sum_{i=1}^{N}\alpha_i^1e^{j\Delta\theta_i}\right|^2\\&=n_tD\left(2^{B_c^I},n_t\right)\left(\sum_{i=1}^{N}\left(\alpha_i^1\right)^2+\sum_{i=1}^{N}\sum_{j=1,j\neq i}^{N}\alpha_i^1\alpha_j^1E\cos\left(\Delta\theta_i-\Delta\theta_j\right)\right)\end{aligned}\tag{17}$$

where the approximate of (a) is derived by using $\mathrm{E}\left|\overline{\mathbf{h}}_i^1\left(\hat{\mathbf{h}}_i^1\right)^H\right|\approx\sqrt{D\left(2^{B_c^I},n_t\right)}$ that is demonstrated in [17]. As θ_i submits the uniform distribution in $[0,2\pi]$ and is quantized uniformly as $\hat{\theta}_i$, $\Delta\theta_i$ is uniformly distributed between $\left[-\pi/2^{B_{PI}},\pi/2^{B_{PI}}\right]$. Then we have [17]

$$\mathrm{E}\left(\cos\left(\Delta\theta_i-\Delta\theta_j\right)\right)=\frac{2^{2B_{PI}}}{\pi^2}\sin^2\left(\frac{\pi}{2^{B_{PI}}}\right),\quad i\neq j\tag{18}$$

Based on the above analysis on average received signal power, the system throughput of the ICS with B_{PI} bits of PI quantization feedback is

$$\begin{aligned}R_{ICS}^1&=\mathrm{E}\log_2\left(1+\rho\left|\sum_{i=1}^{N}\alpha_i^1\mathbf{h}_i^1\hat{\mathbf{v}}_i^1\right|^2\right)\overset{(a)}{\leq}\log_2\left(1+\rho\,\mathrm{E}\left|\sum_{i=1}^{N}\alpha_i^1\mathbf{h}_i^1\hat{\mathbf{v}}_i^1\right|^2\right)\\&\approx\log_2\left(1+\rho n_tD\left(2^{B_c^I},n_t\right)\left(\sum_{i=1}^{N}\left(\alpha_i^1\right)^2+\varphi\left(B_{PI}\right)\sum_{i=1}^{N}\sum_{j=1,j\neq i}^{N}\alpha_i^1\alpha_j^1\right)\right)\end{aligned}\tag{19}$$

where (a) satisfies Jensen's inequality and $\varphi\left(B_{PI}\right)=\frac{2^{2B_{PI}}}{\pi^2}\sin^2\left(\frac{\pi}{2^{B_{PI}}}\right)$. $\varphi\left(B_{PI}\right)$ is an increasing function of B_{PI} when $B_{PI}\geq 0$. As $\varphi\left(B_{PI}=0\right)=0$ and $\varphi\left(B_{PI}\to\infty\right)=1$, the range of $\varphi\left(B_{PI}\right)$ is $[0,1]$. Substitute (9) in (19), the upper bound of the system throughput of the ICS with PI quantization feedback is

$$R_{ICS}^1\leq\log_2\left(1+\rho n_t\left(1-\frac{n_t-1}{n_t}2^{-\frac{B_c^I}{n_t-1}}\right)\left(\sum_{i=1}^{N}\left(\alpha_i^1\right)^2+\varphi\left(B_{PI}\right)\sum_{i=1}^{N}\sum_{j=1,j\neq i}^{N}\alpha_i^1\alpha_j^1\right)\right)\tag{20}$$

For some cell edge user whose single cell gains approximately satisfied $\alpha_1^1=\cdots=\alpha_N^1=\alpha^1$, (20) can be simplified as

$$R_{ICS}^{1-edge} \le \log_2\left(1+\rho N n_t\left(\alpha^1\right)^2\left(1-\frac{n_t-1}{n_t}2^{-\frac{B_c^I}{n_t-1}}\right)\left(1+\left(N-1\right)\varphi\left(B_{PI}\right)\right)\right) \tag{21}$$

According to (20), the upper bound of R_{ICS}^1 is an increasing function of $\varphi\left(B_{PI}\right)$, which illustrates that with more bits for PI feedback, the system throughput would be higher, and the maximum value of R_{ICS}^1 corresponding to $\varphi\left(B_{PI}\right)=1$ is denoted as $R_{ICS}^{1\text{-}max}$,

$$R_{ICS}^{1\text{-}edge-max} \le \log_2\left(1+\rho N^2 n_t\left(\alpha^1\right)^2\left(1-\frac{n_t-1}{n_t}2^{-\frac{B_c^I}{n_t-1}}\right)\right) \tag{22}$$

According to (13) and (22), we get $R_{JCS}^{1-edge} \le R_{ICS}^{1\text{-}edge-max}$. It illustrates that the performance of ICS, benefiting from PI, exceeds JCS. Meanwhile, the feedback of PI increases the overhead of the feedback link. For the feedback link with low capacity, the system throughput shown in (22) is unattainable. But the reasonable feedback-bit allocation between B_c^I and B_{PI} can improve the system throughput. The allocating bits between B_c^I and B_{PI} can be formulated as

$$\begin{aligned}&\max \log_2\left(1+\rho n_t\left(1-\frac{n_t-1}{n_t}2^{-\frac{B_c^I}{n_t-1}}\right)\left(\sum_{i=1}^{N}\left(\alpha_i^1\right)^2+\varphi\left(B_{PI}\right)\sum_{i=1}^{N}\sum_{j=1,j\ne i}^{N}\alpha_i^1\alpha_j^1\right)\right)\\ &s.t.\ B_c^I+B_{PI}=B\end{aligned} \tag{23}$$

where B is the total feedback bits per UE for feeding back CDI and PI.

Notice: The R_{ICS}^1 is an increasing function of B_c^I, and the feedback bits should be real integer, so the resulting B_c^I is given by $\lceil B_c^I \rceil$ or $\lfloor B_c^I \rfloor$ ($\lceil B_c^I \rceil$ or $\lfloor B_c^I \rfloor$ denotes the ceiling or the floor of B_c^I). We can get the optimal solution by exhaustive search of all possible compositions of B since B_c^I and B_{PI} are integer and $B_c^I + B_{PI} = B$.

3.1.2 MU scenario (*K*>1)

In this section, the performance of JCS and ICS for *K*>1 (MU-CoMP) is compared. In this paper, we use ZF precoding to reduce the MU interference. Compiling $\alpha_i^k\left\|\mathbf{h}_i^k\right\|\hat{\mathbf{h}}_i^k\ (k=1,\cdots,K)$ into $\hat{\mathbf{G}}_i=\left[\left(\alpha_i^1\left\|\mathbf{h}_i^1\right\|\hat{\mathbf{h}}_i^1\right)^T,\cdots,\left(\alpha_i^K\left\|\mathbf{h}_i^K\right\|\hat{\mathbf{h}}_i^K\right)^T\right]^T$, the ZF precoding matrix is given by $\hat{\mathbf{V}}_i=\hat{\mathbf{G}}_i^{\dagger}$. The precoding for *k*th UE $\hat{\mathbf{v}}_i^k$ is the normalized vector of the *k*th column of $\hat{\mathbf{V}}_i$.

In MU-CoMP with ZF, CDI feedback is used and the system throughput can be written as

$$R^K=\mathrm{E}\sum_{k=1}^{K}\log_2\left(1+\frac{p\left|\sum_{i=1}^{N}\alpha_i^k\mathbf{h}_i^k\hat{\mathbf{v}}_i^k\right|^2}{\sigma^2+\sum_{t=1,t\ne k}^{K}p\left|\sum_{i=1}^{N}\alpha_i^k\mathbf{h}_i^k\hat{\mathbf{v}}_i^t\right|^2}\right)\approx\sum_{k=1}^{K}\log_2\left(1+\frac{p\mathrm{E}\left|\sum_{i=1}^{N}\alpha_i^k\mathbf{h}_i^k\hat{\mathbf{v}}_i^k\right|^2}{\sigma^2+p\mathrm{E}\sum_{t=1,t\ne k}^{K}\left|\sum_{i=1}^{N}\alpha_i^k\mathbf{h}_i^k\hat{\mathbf{v}}_i^t\right|^2}\right) \tag{24}$$

where the approximation is achieved since we employ the Jensen's inequality to both the numerator and the denominator [20][25]. $\mathrm{E}\left|\sum_{i=1}^{N}\alpha_i^k\mathbf{h}_i^k\hat{\mathbf{v}}_i^k\right|^2$ is computed firstly, as it has no relationship with codeword selection scheme.

$$\begin{aligned}\mathrm{E}\left|\sum_{i=1}^{N}\alpha_i^k\mathbf{h}_i^k\hat{\mathbf{v}}_i^k\right|^2 &= \mathrm{E}\sum_{i=1}^{N}\left|\alpha_i^k\mathbf{h}_i^k\hat{\mathbf{v}}_i^k\right|^2+\mathrm{E}\sum_{i=1}^{N}\sum_{j\neq i}^{N}\alpha_i^k\alpha_j^k\mathbf{h}_i^k\hat{\mathbf{v}}_i^k\left(\mathbf{h}_j^k\hat{\mathbf{v}}_j^k\right)^2\\ &\overset{(a)}{=}\mathrm{E}\sum_{i=1}^{N}\left(\alpha_i^k\right)^2\left|\mathbf{h}_i^k\hat{\mathbf{v}}_i^k\right|^2\overset{(b)}{=}\left(n_t-K+1\right)\sum_{i=1}^{N}\left(\alpha_i^k\right)^2\end{aligned} \tag{25}$$

where (*a*) is derived as $\mathbf{h}_i^k\hat{\mathbf{v}}_i^k$ and $\mathbf{h}_j^k\hat{\mathbf{v}}_j^k$ are independent with each other, $\mathbf{h}_i^k$ and $\hat{\mathbf{v}}_i^k$ are also independent. (*b*) is obtained as $\left|\mathbf{h}_i^k\hat{\mathbf{v}}_i^k\right|^2$ follows a chi-square distribution with $\left(n_t-K+1\right)$ degrees of freedom [26].

For JCS, (24) can be rewritten as

$$R_{JCS}^K\approx K\log_2\left(1+\frac{p\,\mathrm{E}\left|\mathbf{h}^k\hat{\mathbf{v}}^k\right|^2}{\sigma^2+p\,\mathrm{E}\sum_{t=1,t\neq k}^{K}\left|\mathbf{h}^k\hat{\mathbf{v}}^t\right|^2}\right) \tag{26}$$

According to [27], the interference power satisfies

$$\begin{aligned}\mathrm{E}\sum_{t=1,t\neq k}^{K}\left|\mathbf{h}^k\hat{\mathbf{v}}^t\right|^2 &= \left(K-1\right)\mathrm{E}\left(\left\|\mathbf{h}^k\right\|\left\|\hat{\mathbf{v}}^t\right\|\sin^2\theta\cdot\beta\left(1,Nn_t-2\right)\right)\\ &= \left(K-1\right)N\,\mathrm{E}\left\|\mathbf{h}^k\right\|\cdot\mathrm{E}\left(\sin^2\theta\right)\cdot\frac{1}{Nn_t-1}\end{aligned} \tag{27}$$

For JCS, $\left(\sin^2\theta\right)_{JCS}=1-\mathrm{E}\left(\left\|\tilde{\mathbf{h}}^k\left(\hat{\mathbf{h}}^k\right)^H\right\|^2\right)$. Substituting (25) and (27) into (26), we get

$$\begin{aligned}R_{JCS}^K &\approx K\log_2\left(1+\frac{p\left(n_t-K+1\right)\sum_{i=1}^{N}\left(\alpha_i^k\right)^2}{\sigma^2+\dfrac{p\left(K-1\right)N\,\mathrm{E}\left\|\mathbf{h}^k\right\|}{Nn_t-1}\cdot\mathrm{E}\left(\sin^2\theta\right)}\right)\\ &\overset{(a)}{\leq} K\log_2\left(1+\frac{p\left(n_t-K+1\right)\sum_{i=1}^{N}\left(\alpha_i^k\right)^2}{\sigma^2+\dfrac{p\left(K-1\right)N\,\mathrm{E}\left\|\mathbf{h}^k\right\|}{Nn_t-1}\cdot\dfrac{Nn_t-1}{Nn_t}2^{-\frac{NB_c^J}{Nn_t-1}}}\right)\\ &= K\log_2\left(1+\frac{p\left(n_t-K+1\right)\sum_{i=1}^{N}\left(\alpha_i^k\right)^2}{\sigma^2+\dfrac{p\left(K-1\right)\mathrm{E}\left\|\mathbf{h}^k\right\|}{n_t}2^{-\frac{NB_c^J}{Nn_t-1}}}\right)\end{aligned} \tag{28}$$

where step (a) is arrived at by using (9).

For MU-CoMP with ZF precoding, the signal is mainly determined by the degrees of freedom, while the interference is related to the quantization error $\sin^2\theta$. Therefore, $\sin^2\theta$ in ICS is different from that in JCS, which is denoted as

$$\left(\sin^2\theta\right)_{ICS} = 1 - \mathrm{E}\left(\left|\sum_{i=1}^{N}\left(g_i^k\right)^2 \overline{\mathbf{h}}_i^k \left(\hat{\mathbf{h}}_i^k\right)^H\right|^2\right) \tag{29}$$

Similar as (17), $\mathrm{E}\left(\left|\sum_{i=1}^{N}\left(g_i^k\right)^2 \overline{\mathbf{h}}_i^k \left(\hat{\mathbf{h}}_i^k\right)^H\right|^2\right)$ is computed as

$$\begin{aligned}\mathrm{E}\left(\left|\sum_{i=1}^{N}\left(g_i^k\right)^2 \overline{\mathbf{h}}_i^k \left(\hat{\mathbf{h}}_i^k\right)^H\right|^2\right) &= \mathrm{E}\left|\sum_{i=1}^{N}\left(g_i^k\right)^2 \left|\overline{\mathbf{h}}_i^k \left(\hat{\mathbf{h}}_i^k\right)^H\right| e^{j\Delta\theta_i}\right|^2 \\ &= D\left(2^{B_c^I}, n_t\right)\left(\sum_{i=1}^{N}\left(g_i^k\right)^4 + \varphi\left(B_{PI}\right)\sum_{i=1}^{N}\sum_{j=1,\, j\neq i}^{N}\left(g_i^k g_j^k\right)^2\right)\end{aligned} \tag{30}$$

The system throughput of the ICS with per-cell codebook is

$$R_{ICS}^K \le K\log_2\left(1 + \frac{p\left(n_t - K + 1\right)\sum_{i=1}^{N}\left(\alpha_i^k\right)^2}{\sigma^2 + \dfrac{p\left(K-1\right)N\,\mathrm{E}\left\|\mathbf{h}^k\right\|}{Nn_t - 1}\overline{\left(\sin^2\theta\right)}_{ICS}}\right) \tag{31}$$

where $\overline{\left(\sin^2\theta\right)}_{ICS} = 1 - \left(1 - \dfrac{n_t - 1}{n_t}2^{-\frac{B_c^I}{n_t - 1}}\right)\left(\sum_{i=1}^{N}\left(g_i^k\right)^4 + \varphi\left(B_{PI}\right)\sum_{i=1}^{N}\sum_{j=1,\, j\neq i}^{N}\left(g_i^k g_j^k\right)^2\right)$.

For some cell edge user whose single cell gains approximately satisfied $\alpha_1^k = \cdots = \alpha_N^k = \alpha^k$, (28) and (31) can be simplified as

$$\begin{aligned}R_{JCS}^{K-edge} &\le K\log_2\left(1 + \frac{pN\left(n_t - K + 1\right)\left(\alpha^k\right)^2}{\sigma^2 + pN\left(K-1\right)\left(\alpha^k\right)^2 2^{-\frac{NB_c^I}{Nn_t - 1}}}\right) \\ R_{ICS}^{K-edge} &\le K\log_2\left(1 + \frac{pN\left(n_t - K + 1\right)\left(\alpha^k\right)^2}{\sigma^2 + \dfrac{pN^2 n_t\left(K-1\right)\left(\alpha^k\right)^2}{Nn_t - 1}\overline{\left(\sin^2\theta\right)}_{ICS}^{edge}}\right)\end{aligned} \tag{32}$$

where $\overline{\left(\sin^2\theta\right)}_{ICS}^{edge} = 1-\left(1-\frac{n_t-1}{n_t}2^{-\frac{B_c^I}{n_t-1}}\right)\left(\frac{1+(N-1)\varphi(B_{PI})}{N}\right)$.

Similar as (23), the feedback-bit allocation between B_c^I and B_{PI}, with the fixed total number of feedback bits, to maximize the R_{ICS}^K is given by

$$\max \frac{p(n_t-K+1)\sum_{i=1}^{N}\left(\alpha_i^k\right)^2}{\sigma^2+\frac{p(K-1)N\,\mathrm{E}\left\|\mathbf{h}^k\right\|}{Nn_t-1}\overline{\left(\sin^2\theta\right)}_{ICS}} \quad (33)$$

$$s.t.\ B_c^I + B_{PI} = B.$$

3.2 Feedback Overhead and Selection Complexity Analysis

For convenient comparison, we assume $B_c = B_c^J = B_c^I$ in this section.

For JCS, each BS need B_c for CDI feedback, besides that, each BS need extra B_{PI} overhead for ICS with PI. Therefore, the feedback overhead for the two schemes are NB_c and $N(B_c+B_{PI})$ in the N cooperation BSs conditions.

According to the codeword selection criterions shown in (6), the quantized vector for each BS is selected from 2^{B_c} codewords and the quantization for N cooperation BSs is independently, so the selection complexity of ICS with PI is $N2^{B_c}$. In the case of JCS, it has exponential complexity w.r.t. the codebook size as shown in (7). Since there are $\left(2^{B_c}\right)^N$ codeword combinations, the selection complexity of JCS is 2^{NB_c}.

Feedback overhead and selection complexity of two codeword selection schemes are summarized in **Table 1**, and JCS is used as the baseline to calculate the gain of feedback overhead and selection complexity for ICS with PI.

Table 1. Feedback overhead and selection complexity of two codeword selection schemes

	Feedback overhead	**Gain of feedback overhead**	**Selection complexity**	**Gain of selection complexity**
JCS	NB_c	--	2^{NB_c}	--
ICS with PI	$N(B_c+B_{PI})$	$\frac{B_{PI}}{B_c}$	$N2^{B_c}$	$\frac{N2^{B_c}-2^{NB_c}}{2^{NB_c}}$

Table 2. Example of Feedback overhead and selection complexity of two codeword selection schemes

	Feedback overhead	**Gain of feedback overhead**	**Selection complexity**	**Gain of selection complexity**
JCS	12	--	4096	--
ICS with PI	18	50.0%	48	-98.8%

4. Simulation Results and Analysis

In this section, we compare the system throughput of ICS and JCS via numerical and simulation results. In the evaluation, In the evaluation, path loss is modeled as $\alpha = r^{-\theta}$. r is the distance between the BS and user, and θ is the path loss coefficient ($\theta = 2$ is assumed in this paper). we set $n_t = 4$ and the impact of different value of SNR ρ, the number of cooperation BSs N, the number of bits for PI feedback B_{PI} to the system throughput is considered.

4.1 System Throughput with K=1

Fig. 2 show the comparison between the practical throughput and the theoretical upper bound of system throughput of JCS and ICS with PI feedback. Both the figures are plotted with varying SNR ρ when $N = 3$ and $B_c^J = B_c^I = 4$. It is observed that the practical throughput is close to the theoretical throughput upper bound both for JCS and ICS. **Fig. 3** verifies the comparison under different number of cooperation BSs with $\rho = 5$ dB and $B_c^J = B_c^I = 4$. They prove the availability of the throughput upper bound.

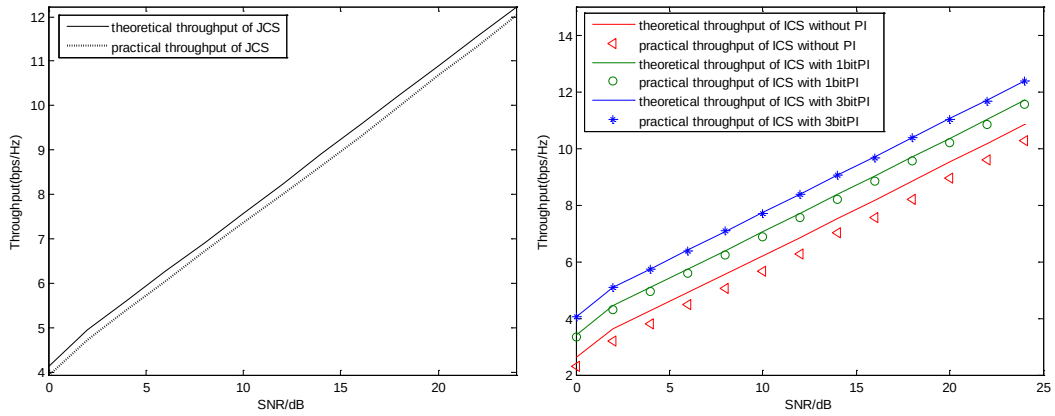

Fig. 2. Comparison between practical throughput and theoretical throughput upper bound versus SNR when $N = 3$, $B_c^J = B_c^I = 4$.

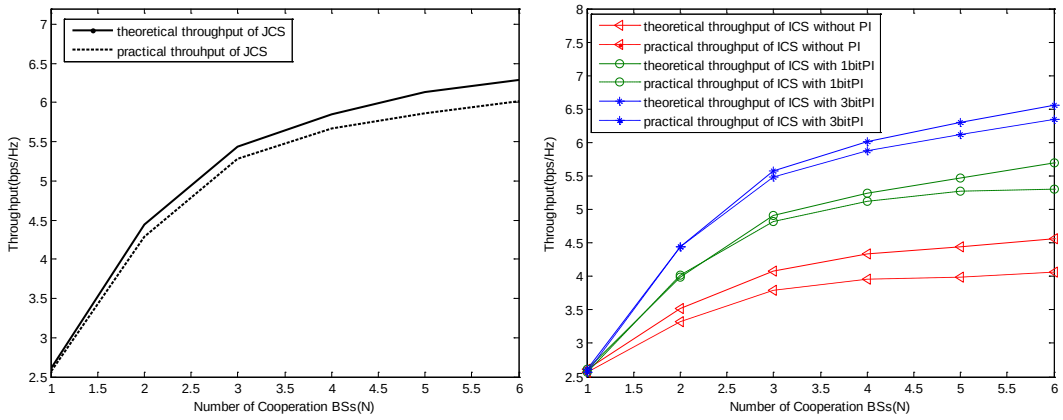

Fig. 3. Comparison between practical throughput and theoretical throughput upper bound versus number of cooperation BSs when $\rho = 5$, $B_c^I = B_c^I = 4$.

The performance of R_{ICS}^{1} with different number of B_{PI} and R_{JCS}^{1} are compared in **Fig. 4** when $B_c^J = B_c^I = 4$ and $\rho = 5\,\text{dB}$. The results illustrate the benefit of PI feedback well, and shows that the ICS with two bits PI for coordinated BSs can achieve the approximate throughput with JCS.

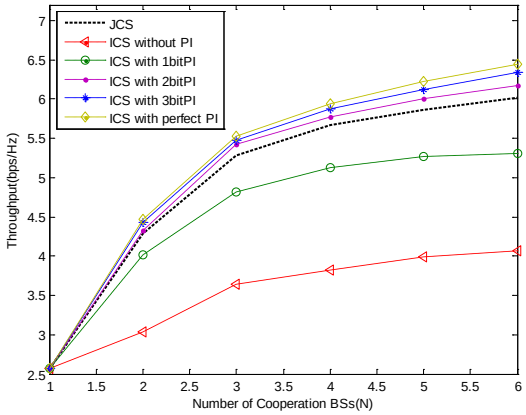

Fig. 4. Throughput of R_{ICS}^{1} with different number of B_{PI} and R_{JCS}^{1} when $n_t = 4$, $B_c^J = B_c^I = 4$.

With the increase of the number of cooperation BSs, the gap between ICS without PI and JCS becomes larger. This result shows that, in the ICS without PI, the difference on PI of each cooperation BS impedes the throughput increasing. With PI feedback, the throughput of ICS increase greatly, which makes the throughput gain is more obvious when the cooperation BSs numbers increase.

With the fix feedback bits, **Fig. 5** depicts the effect of feedback-bit allocation to system throughput when $\rho = 5\,\text{dB}$, assuming the same amount of feedback bits for JCS and ICS, i.e. $B_c^J = B_c^I + B_{PI} = 4$. The blue line is throughput of ICS with feedback-bit allocation, which follows the criterion of (23). Via optimal feedback-bit allocation, ICS can greatly enhance the system throughput with no additional feedback overhead, i.e. about 32.5% when *N*=3, and the improvement will be enhanced when the cooperation BSs' number increases. However, with the same amount of feedback bits, ICS still cannot surpass JCS.

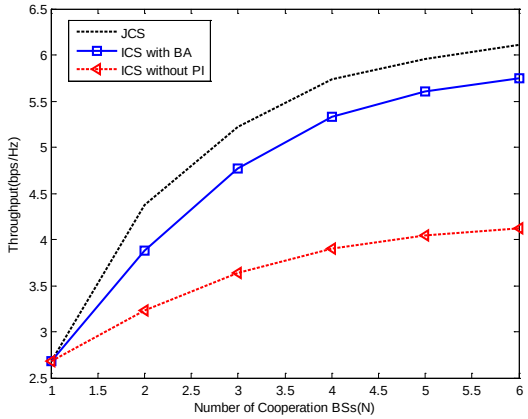

Fig. 5. Throughput of R_{JCS}^{1} and R_{ICS}^{1} with bits allocation between B_c^I and B_{PI} when $n_t = 4$, $B_c^J = B_c^I + B_{PI} = 4$.

4.2 System Throughput with K>1

Corresponding to the situation of K=1, the comparison between the practical throughput and the theoretical throughput upper bound for JCS and ICS with PI feedback are shown in **Fig. 6**. Both the figures are plotted with varying SNR ρ when $N=3$, K=3 and $B_c^J = B_c^I = 4$. **Fig. 7** verifies the comparison under different number of cooperation BSs with $\rho = 5$ dB, K=3 and $B_c^J = B_c^I = 4$. The simulation results demonstrate the validity of the theoretical analysis.

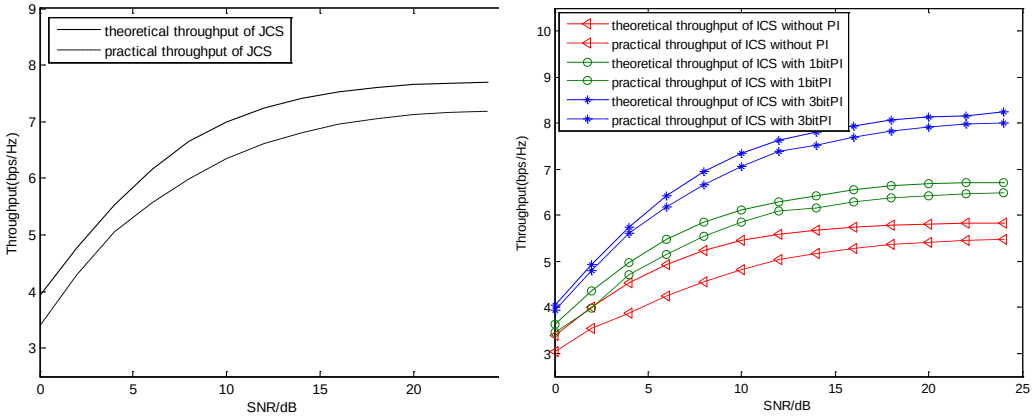

Fig. 6. Comparison between practical throughput and theoretical throughput upper bound versus SNR when $N=3$, $B_c^J = B_c^I = 4$, $K=3$.

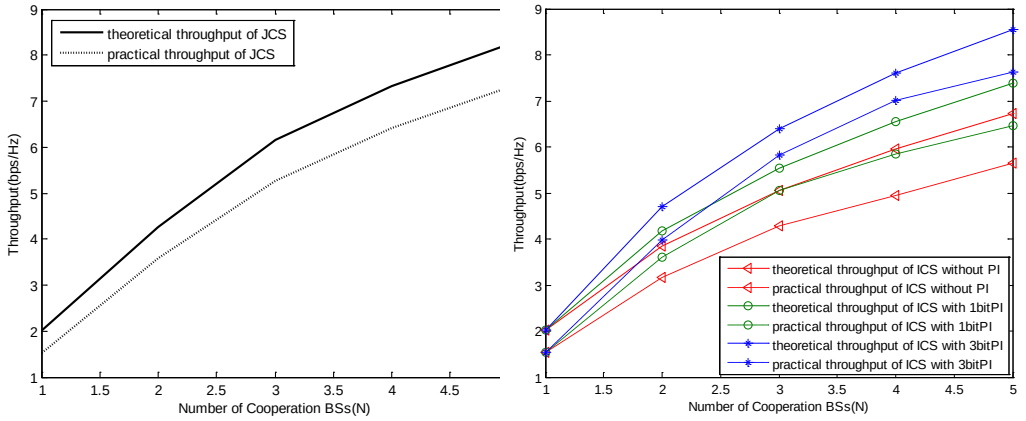

Fig. 7. Comparison between practical throughput and theoretical throughput upper bound versus number of cooperation BSs when $\rho = 5$, $B_c^J = B_c^I = 4$, $K=3$.

In **Fig. 8**, the performance comparison between R_{ICS}^K with different number of B_{PI} and R_{JCS}^K is given when $\rho = 5$ dB, $B_c^J = B_c^I = 4$ and K=3. It also shows that the number of the cooperation BSs has the effect on the difference between these schemes. **Fig. 9** verifies the effectiveness of bits allocation to B_c^I and B_{PI} with the criterion shown in (13). The results are derived under the same assumption as Fig.12 except for $B_c^J = B_c^I + B_{PI} = 4$.

Since **Fig. 8** and **Fig. 9** have the same tendency as **Fig. 4** and **Fig. 5**, we can obtain the similar conclusions. JCS is superior in throughput. With the same amount of feedback bits, ICS, employing feedback-bit allocation strategy between CDI and PI, still cannot surpass JCS.

Only with the additional PI feedback, ICS will outperform JCS when the number of bits for PI exceed two, as shown in **Fig. 4** and **Fig. 8**. Therefore, the scheme of ICS with PI can be regarded as a tradeoff scheme between JCS and ICS in system throughput.

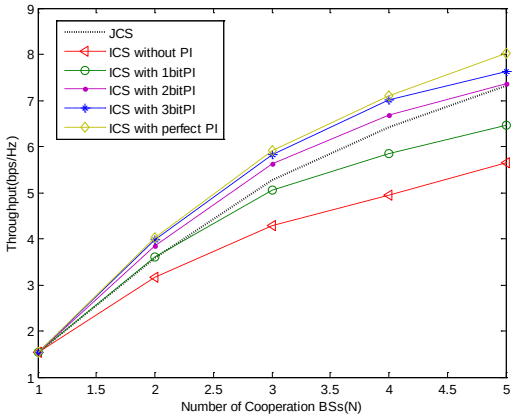

Fig. 8. Throughput of R_{ICS}^{K} with different number of B_{PI} and R_{JCS}^{K} when $n_t = 4$, $B_c^J = B_c^I = 4$, $K = 3$.

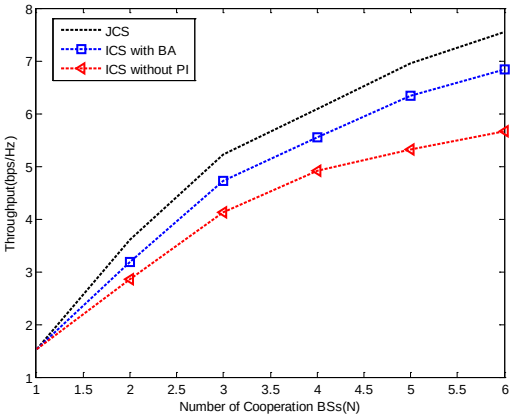

Fig. 9. Throughput of R_{JCS}^{K} and R_{ICS}^{K} with bits allocation between B_c^I and B_{PI} when $n_t = 4$, $B_c^J = B_c^I + B_{PI} = 4$, $K = 3$.

From theoretical analysis and the simulation results shown in the **Fig. 4**, **Fig. 5**, **Fig. 8** and **Fig. 9**, we have the following conclusions.

- By comparing the criterion of (6) and (7), the ICS obviously has lower complexity of codeword selection, but its system throughput is poor without PI feedback. Therefore, ICS with PI can be seen as a tradeoff scheme between ICS and JCS in system throughput.
- With the same amount of feedback bits, the system throughput obtained by JCS is much higher. The system throughput of ICS will be increased by allocating feedback bits between B_c^I and B_{PI}, but ICS is still inferior to JCS, as shown in **Fig. 5** and **Fig. 9**.
- With additional feedback bits of PI feedback, ICS can significantly improve the system throughput. With the same codebook size for CDI quantization, the system throughput of ICS with PI feedback will outperform JCS when the feedback bits of PI exceed two bits for coordinated BSs, as shown in **Fig. 4** and **Fig. 8**. However, the PI feedback will increase feedback overhead with the number of coordinated BSs linearly.

- Without considering of the selection complexity, JCS has a better tradeoff between system throughput and feedback overhead.

5. Conclusion

In this paper, we study the codeword selection schemes for per-cell codebook in CoMP limited feedback system. The upper bounds of system throughput achieved by ICS and JCS are analyzed. Several respects of ICS and JCS, including feedback overhead, selection complexity and system throughput, are compared. The theoretical analysis and the simulation results show that JCS is a better choice for system performance and feedback overhead. The ICS has obvious advantage with lower complexity, but it needs additional PI feedback if it obtains the same system throughput of JCS. Under the same number of feedback bits constraint, allocating the number of feedback bits for CDI and PI quantization can increase the system throughput, but ICS is still inferior to JCS.

JCS is a better choice for system performance and feedback overhead but the exponential complexity of codeword selection w.r.t. the codebook size. This disadvantage makes JCS have limitation in the practical application. So we should give some methods to reduce the complexity of JCS. Reducing the size of the per-cell codebook before joint selection shown in (7) is a simple way to solve this problem. The specific criterion for the codebook size reduction can refer to [12], which decreases the selection complexity of JCS greatly with tiny loss on performance and no additional feedback overhead. As to the situation of allowing only low-complexity for codeword selection at UE, ICS with PI can be considered with bit allocation strategy [18].

References

[1] F. Rusek, D. Persson, B. K. Lau, E. G. Larsson, T. L. Marzetta, O. Edfors, and F. Tufvesson, "Scaling up MIMO: opportunities and challenges with very large arrays," *IEEE Signal Processing Magazine*, vol. 30, no. 1, pp. 40-46, January, 2013. Article (CrossRef Link).

[2] X. H. You, D. M. Wang, B. Sheng, X. Q. Gao, X. S. Zhao, and M. Chen, "Cooperative distributed antenna systems for mobile communications [Coordinated and Distributed MIMO]," *IEEE on Wireless Communications*, vol. 17, no. 3, pp. 35-43, June, 2010. Article (CrossRef Link).

[3] M. Sawahashi, Y. Kishiyama, A. Morimoto, D. Nishikawa, and M. Tano, "Coordinated multipoint transmission/reception techniques for LTE-advanced [Coordinated and Distributed MIMO]," *IEEE on Wireless Communications*, vol. 17, no. 3, pp. 26-34, June, 2010. Article (CrossRef Link).

[4] D. Lee, H. Seo, B. Clerckx, E. Hardouin, D. Mazzarese, S. Nagata and K. Sayana, "Coordinated multipoint transmission and reception in LTE-advanced: deployment scenarios and operational challenges," *IEEE Commu. Mag.*, vol. 50, no. 2, pp. 148-155, 2012. Article (CrossRef Link).

[5] Tae Min Kim, Fan Sun and A. J. Paulraj, "Low-Complexity MMSE precoding for coordinated multipoint with per-antenna power constraint," *IEEE Signal Processing Letters*, vol. 20, no. 4, pp. 395-398, April 2013. Article (CrossRef Link).

[6] Fan Sun and De Carvalho. E, "A leakage-based MMSE beamforming design for a MIMO interference channel," *IEEE Signal Processing Letters*, vol. 19, no. 6, pp. 368-371, June, 2012. Article (CrossRef Link).

[7] K. Rantelobo, Wirawan, G. Hendrantoro, A. Affandi and H. A. Zhao, "Adaptive combined scalable video coding over MIMO-OFDM systems using partial channel state information," *KSII Transactions on Internet and Information Systems*, vol. 7, no. 12, pp. 3200-3219, December, 2013. Article (CrossRef Link).

[8] D. J. Love, R. W. Heath, V. K. N. Lau, D. Gesbert, B. D. Rao, and M. Andrew, "An overview of limited feedback in wireless communication systems," *IEEE Journal Select Areas*

Communications, vol. 26, pp. 1341-1365, October, 2008. Article (CrossRef Link).
[9] D. Su, X. Y. Hou and C. Y. Yang, "Quantization based on per-cell codebook in cooperative multi-cell systems," in *Proc. of IEEE Wireless Communications and Networking Conference (WCNC)*, pp. 1753-1758, March 2011. Article (CrossRef Link).
[10] J. H. Kim, W. Zirwas and M. Haardt, "Efficient feedback via subspace-based channel quantization for distributed cooperative antenna systems with temporally correlated channels," *EURASIP J. Adv. Signal Process*, vol. 2008, no. 2, pp. 1-13, January, 2008. Article (CrossRef Link).
[11] Y. Cheng, V. K. N. Lau and Y. Long, "A scalable limited feedback design for network MIMO using per-cell product codebook," *IEEE Transactions on Wireless Communications*, vol. 9, no. 10, pp. 3093-3099, October, 2010. Article (CrossRef Link).
[12] Z. R. Hu, T. K. Zhang and C. Y. Feng, "Study on codeword selection for per-cell codebook with limited feedback in CoMP systems," in *Proc. of IEEE Wireless Communications and Networking Conference (WCNC)*, pp. 3140-3145, April, 2013. Article (CrossRef Link).
[13] E. Zeng, S. Zhu, and M. Xu, "Impact of limited feedback on multiple relay zero-forcing precoding systems," *IEEE International Conference on Communications*, pp. 4992-4997, May, 2008. Article (CrossRef Link).
[14] E. Zeng, S. Zhu, X. Liao and Z. Zhong, "Impact of limited feedback on the performance of MIMO macrodiversity transmission," in *Proc. of IEEE Wireless Communications and Networking Conference (WCNC)*, pp. 672-677, March, 2008. Article (CrossRef Link).
[15] F. Yuan and C. Y. Yang, "Phase ambiguity quantization for per-cell codebook based limited feedback coordinated multi-point transmission systems," in *Proc. of IEEE Vehicular Technology Conference (VTC)*, 2011. Article (CrossRef Link).
[16] M. H. Hassan, Y. A. Fahmy and M. M. Khairy, "Phase ambiguity mitigation for per-cell codebook based limited feedback coordinated multi-point transmission systems," *IET Communications*, vol. 6, no. 15, pp. 2378- 2386, October, 2012. Article (CrossRef Link).
[17] D. Su and C. Y. Yang, "Necessity of phase ambiguity quantization for limited feedback coordinated multi-point transmission," *IEEE Vehicular Technology Conference (VTC)*, September, 2011. Article (CrossRef Link).
[18] F. Yuan and C. Y. Yang, "Bit allocation between per-Cell codebook and phase ambiguity quantization for limited feedback coordinated multi-point transmission systems," *IEEE Transactions on Communications*, vol. 60, no. 9, pp. 2546-2559, September, 2012. Article (CrossRef Link).
[19] S. Yu, H. B. Kong, Y. T. Kim, S. H. Park and I. Lee, "Novel feedback bit allocation methods for multi-cell joint processing systems," *IEEE Transactions on Wireless Communications*, vol. 11, no. 9, pp. 3030-3036, September, 2012. Article (CrossRef Link).
[20] Y. L. Wu, M. Ding, J. Zou and X. N. Li, "Efficient limited feedback for MIMO-Relay systems," *IEEE Communication Letters*, vol. 15, no. 2, February, 2011. Article (CrossRef Link).
[21] X. R. Xu, Y. D. Yao, S. Q. Hu and Y. B. Yao, "Joint subcarrier and bit allocation for secondary user with primary users' cooperation," *KSII Transactions on Internet and Information Systems*, vol. 7, no. 12, pp. 3037-3054, December, 2013. Article (CrossRef Link).
[22] B. Khoshnevis and Y. Wei, "Bit allocation laws for multiantenna channel feedback quantization: multiuser case," *IEEE Transactions on Signal Processing*, vol.60, no.1, pp.367-382, January, 2012. Article (CrossRef Link).
[23] E. Park, H. Kim, H. Park and I. Lee, "Feedback bit allocation schemes for multi-user distributed antenna systems," *IEEE Communication Letters*, vol. 17, no. 1, 2013. Article (CrossRef Link).
[24] C. Au-Yeung and D. J. Love, "On the performance of random vector quantization limited feedback beamforming in a MISO system," *IEEE Transactions on Wireless Communications*, vol. 6, no. 2, pp. 458-462, February, 2007. Article (CrossRef Link).
[25] S. Q. Han and C. Y. Yang, "Downlink multicell cooperative transmission with imperfect CSI sharing," in *Proc. of IEEE International Conference on Acoustics, Speech and Signal Processing (ICASSP)*, pp. 3024-3027, 2011. Article (CrossRef Link).
[26] J. Zhang, R. W. Heath, M. Kountourix and J. G. Andrews, "Mode switching for the multi-antenna broadcast channel based on delay and channel quantization," *EURASIP Journal on Advances in*

Signal Processing, vol. 2009, no. 1, pp. 1-15, 2009. Article (CrossRef Link).
[27] T. Yoo, N. Jindal and A. Goldsmith, "Multi-antenna downlink channels with limited feedback and user selection," *IEEE Journal Select Areas Communications*, vol. 25, no. 8, pp. 1478-1491, September, 2007. Article (CrossRef Link).

Zhirui Hu is currently pursuing the Ph.D. degree in Communication and Information Systems at Beijing University of Posts and Telecommunications (BUPT). Her current research field is in the areas of wireless communications, multiple-antenna technology, cooperative communications and signal processing technology.

Chunyan Feng received the B.S. degree in Communications Engineering, the M.S. and Ph.D. degrees in Communication and Information Systems, all from Beijing University of Posts and Telecommunications (BUPT), Beijing, China. She is currently a Professor with the School of Information and Communication Engineering, BUPT. Her research interests are in the areas of broadband networks and wireless communication systems. Current research focuses on cognitive radio, key technology of B3G/4G systems, and green wireless communications.

Tiankui Zhang BSc(Eng), PhD is a associate professor at the School of Informationand Communication Engineering of Beijing University of Posts and Telecoms(BUPT). He received his BEng and PhD degrees from BUPT, in the areas of Wireless Telecommunications in the years 2003 and 2008 respectively. His research field is in the areas of next generation wireless networks with particular focus on radio resource management and green radio.

Qiubin Gao received his B.S. and Ph.D. in control science and engineering from Tsinghua University. He is currently a senior research engineer at Datang Wireless Mobile Innovation Center of China Academy of Telecommunication Technology (CATT). His current research interests include physical layer design for mobile communication, multiple-antenna technology, CoMP, and system performance evaluation. He is inventor /co-inventor of more than 100 patents in wireless communications, and author/co-author of a number journal and conference papers.

Shaohui Sun received a B.S. with auto control engineering and M.S. with computer engineering from Xidian University in 1994 and 1999, respectively, and a Ph.D. in communication and information system from Xidian University in 2003. He has been deeply involved in the development and standardization of LTE/LTE-Advanced since 2005. His research area of interest includes multiple-antenna technology, heterogeneous wireless network and relay.